Gondwana Research 36 (2016) 376–389

Contents lists available at ScienceDirect

Gondwana Research

journal homepage: www.elsevier.com/locate/gr

Topographic architecture and drainage reorganization in Southeast China: Zircon U-Pb chronology and Hf isotope evidence from Taiwan

Qing Lan [a,b], Yi Yan [a,*], Chi-Yue Huang [a,c], M. Santosh [d], Ye-Hua Shan [a], Wenhuang Chen [a,e], Mengming Yu [a,e], Kun Qian [a,e]

[a] Key Laboratory of Marginal Sea Geology, Guangzhou Institute of Geochemistry, Chinese Academy of Sciences, Guangzhou, China
[b] State Key Laboratory of Ore Deposits Geochemistry, Institute of Geochemistry, Chinese Academy of Sciences, Guiyang, China
[c] Department of Earth Sciences, National Cheng Kung University, Tainan, Taiwan
[d] Journal Center, School of Earth Sciences and Resources, China University of Geosciences, Beijing China
[e] College of Earth Science University of Chinese Academy of Sciences, Beijing, China

ARTICLE INFO

Article history:
Received 1 March 2015
Received in revised form 28 April 2015
Accepted 2 July 2015
Available online 14 August 2015

Handling Editor: W.J. Xiao

Keywords:
East Tibet
Provenance
Topography
Drainage system
Zircon geochronology

ABSTRACT

The uplift of Tibet Plateau and the marginal sea spreading have had important influence on the tectonic, landform and drainage system in East Asia, although the marginal sea spreading in shaping the topography and drainage reorganization in East Asia has been still controversial. Here we present U-Pb age and Hf isotopic composition of detrital zircon grains from Cenozoic sedimentary rocks in Taiwan to understand how the provenance and river systems evolved. Our data show that the U-Pb age spectra of detrital zircon grains in Paleogene sandstones are dominated by Yanshanian (180–67 Ma) zircon grains and with subordinate or nil Proterozoic and Archean zircon grains. These results are in contrast to those in Miocene rocks that are dominated by the Indosinian (257–205 Ma) zircon grains together with Yanshanian, Proterozoic and Archean population. The initial Hf isotope ratios [$\varepsilon Hf(t)$] of the zircon grains also display systematic change in Paleogene and Neogene strata. Our data demonstrate that the Hsuehshan Range and Western Foothills in Taiwan have the same sedimentary sources. The source region of Paleogene strata was mainly located at the coast in southeast China and migrated inland over time. The source might have reached the Lower Yangtze region during early Miocene. Although the mechanism of transport of sediments from the Lower Yangtze region to Taiwan is unclear, we speculate that the Minjiang River might have been larger in Early Miocene than the present and might have delivered inland material along the boundary of Yangtze and Cathaysia Blocks to Taiwan. These were then captured by the Yangtze River systems at some time after Late Miocene. This change corresponds to the time of the drainage reorganization in East Tibet, such as Yangtze River, and the regional subsidence resulting from the opening of marginal sea. The combined effects of Tibet uplift and opening of marginal sea might have shaped the topography and river system reorganization in East Tibet. The evolution of topography and drainage systems in southeast China seems to be mainly controlled by the opening of marginal sea.

1. Introduction

The interaction among tectonics, landforms and drainage systems in East Asia has been the focus of several recent studies (Clark et al., 2004, 2005; Clift et al., 2006; Yan et al., 2011; Zheng et al., 2013; Robinson et al., 2014). The uplift of Tibet Plateau and the opening of marginal sea are among the major tectonic events in East Tibet area. The thermochronological data from the eastern margin of the plateau suggest an important period of plateau margin growth during Cenozoic (Wang et al., 2012). Meanwhile, large-scale rift systems developed in southeast China during Late Mesozoic-Early Cenozoic (Yao et al., 1994), which finally led to the formation of a series of rifted basins and culminated in the opening of marginal seas, such as South China Sea during the Paleogene (Taylor and Hayes, 1980; Briais et al., 1993; Lan et al., 2014). During the transition from rifting to seafloor spreading, a series of breakup unconformities develops in the rifted basins in northern margin of South China Sea (Zhou et al., 1995; Lin et al., 2003; Lan et al., 2014). The diachronous westward younging of these breakup unconformities is consistent with seafloor spreading propagating from east to west (Lan et al., 2014). Although the surface uplift of Tibetan Plateau is believed to have significantly influenced the tectonics, landforms and drainage systems during the Cenozoic in East Asia (Harrison et al., 1992; Burchfiel et al., 1995; Fielding, 1996; Wang, 1998; Li and Fang, 1999; Wang, 2004), the role of marginal sea spreading in shaping the topography of East Asia has yet to be further studied.

The evolution of large drainages such as the Yangtze River has been used to constrain the establishment of topography in large area (Clark et al., 2005; Clift et al., 2006). The evidence of Nd isotope and the detrital zircon grains from the Hanoi Basin, Central Myanmar and lower Yangtze

* Corresponding author. Tel.: +86 20 85290212.
E-mail address: yanyi@gig.ac.cn (Y. Yan).

http://dx.doi.org/10.1016/j.gr.2015.07.008
1342-937X/

suggest that the establishment of the modern drainage systems in East Tibet prior to 23 Ma (Clift et al., 2006; Zheng et al., 2013; Robinson et al., 2014), even though some workers consider that the Yangtze River is younger than 5 Ma (Li et al., 2001; Yang and Youn, 2007; Jia et al., 2010). However, the evolutionary features of river systems in southeast China, such as the Minjiang River (Fig. 1), are scarcely taken into consideration. What was their relationship with Yangtze River, and how did the opening of marginal seas affect their evolution are still ambiguous.

The changes in river discharge must have had a major influence on the offshore sedimentary rocks in passive continental margin of southeast China, which can provide spatial and temporal constraints on the development of regional drainage systems (Clift et al., 2002; Li et al., 2003; Richardson et al., 2011). However, the difficulty in obtaining samples inhibits a better understanding. Based on the study of Nd isotopes of sediments in the northern margin of South China Sea (ODP Site 1148) (Fig. 1), Clift et al. (2002) interpreted the provenance of northern margin of South China Sea as the northern source accompanied by

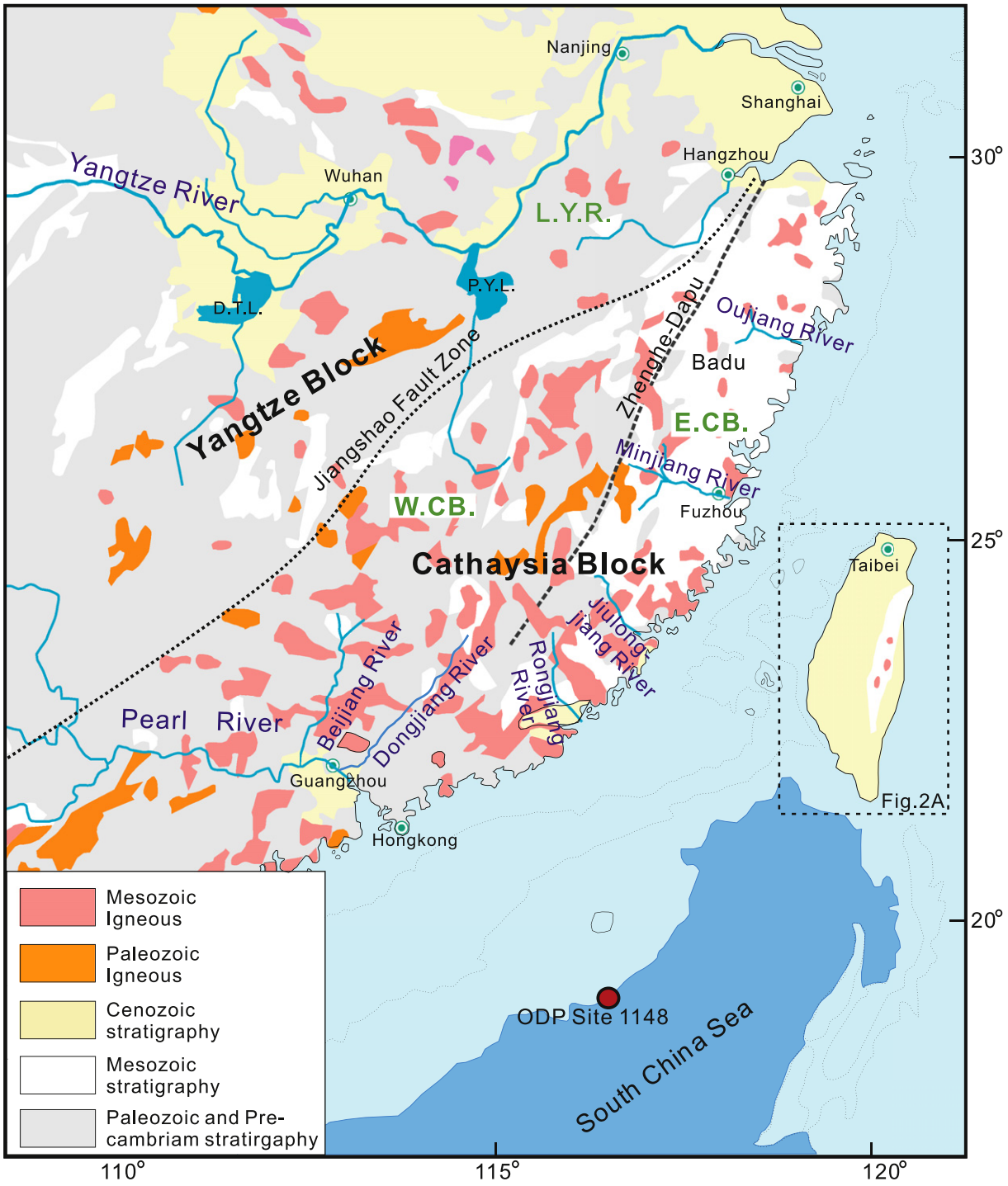

Fig. 1. Simplified geological map of southeast China and distribution of main river systems. The Cathaysia Block has been broadly subdivided into the western and eastern parts along the Zhenghe-Dapu fault according to Chen and Jahn (1998) and Xu et al. (2007). Abbreviations: L.Y.R.: Lower Yangtze Region. E.Ca. and W.Ca: East and West Cathaysia Block. P.Y.L.: PoYang Lake. D.T.L.: Dong Ting Lake.

gradual inland erosion, which is consistent with the study in Pearl River Mouth Basin (Shao et al., 2007). From the same drill site, however, Li et al. (2003) arrived at a different conclusion that demonstrated two major provenances. These are the pre-27 Ma southwestern source region such as the Indochina-Sunda Shelf and Borneo and the post-23 Ma northern provenance in South China. This controversy concerns the understanding of the mechanism that controls the evolution of sedimentary source.

The thick and successive Cenozoic sedimentary sequences on the continental margin of southeast China were deformed, uplifted and exposed along the Western Foothills and Hsuehshan Range of Taiwan (Fig. 2) during mountain building resulting from arc-continent collision after 6.5 Ma (Suppe, 1984; Huang et al., 1997; Huang et al., 2000). This region provides an excellent opportunity for sampling without expensive oceanic drilling. Therefore, Taiwan is the best window to gain insights on the evolution of topography and early river systems in eastern China.

The study of Yokoyama et al. (2007) on the detrital monazite grains from Taiwan showed a complex material source for the Cenozoic rocks. For example, the provenance of sediments in Western Foothills indicated that the major source region such as Korean Peninsula, Shandong Peninsula and Fujian Province, but the Eocene and Oligocene strata of the Hsuehshan Range were sourced from an area that was within the drainage basins of the modern Pearl River. However, data from stratigraphy and sedimentology consistently indicated northwestern or western source region for the Western Foothills and Hsuehshan Range (Chou, 1977; Tan and Youh, 1978; Chou, 1980). Thus, the source region for Cenozoic strata in Taiwan is critical to evaluate the tectonic implications.

The U-Pb geochronology of detrital zircon grains in sandstones have been widely employed to trace provenance (Gaudette et al., 1981; Miller and Saleeby, 1995; Rainbird et al., 1997; Duan et al., 2011) and offers a better tool than the neodymium isotopes of mudstones, which can only provide an estimate of the mixed components source region (McLelland et al., 1993; McLennan et al., 2001). In this study, we discussed the provenances of Cenozoic rocks exposed in the Western Foothills and Hsuehshan Range using U-Pb age spectra and Hf isotope of detrital zircon grains from Cenozoic sandstones in Taiwan. In particular, we address (1) the comparison of sedimentary source for the Paleogene stratigraphy in Western Foothills and Hsuehshan

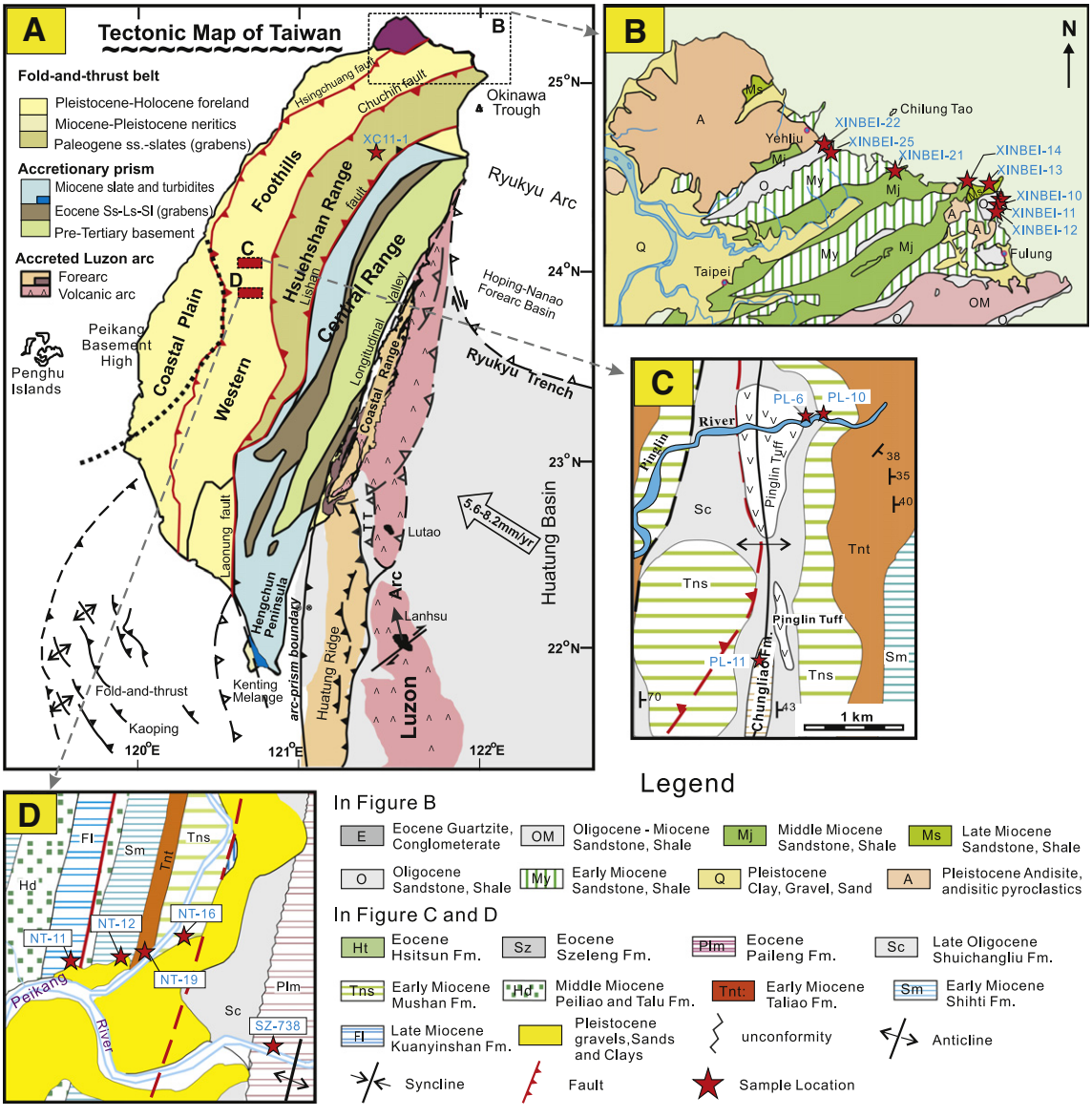

Fig. 2. Tectonic Map of Taiwan (A) and sample section in northern and central Taiwan (B, C, D).

Range, (2) the provenance evolution and its tectonic implication for the Tertiary strata in Taiwan, and (3) the tectonics control on the early evolution of the regional fluvial systems and topography framework.

2. Geological background

The Taiwan Island is situated at the boundary between the Eurasian Plate and the Philippine Sea Plate (Fig. 1). The South China Sea subducted along the Manila Trench beneath Philippine Sea Plate starting from ca.15 Ma, which was accompanied by volcanism in the Luzon Arc (Briais et al., 1993; Yang et al., 1996). Meanwhile, the Eurasian passive continental margin sedimentary sequences were deformed, uplifted and exposed along Western Foothills and Hsuehshan Range on Taiwan Island resulting from the collision of the Luzon volcanic arc with the Eurasian passive continental margin at a relative convergence velocity of 70–80 km/Ma (Seno et al., 1993).

Taiwan can be divided into the Coastal Plain, Western Foothills, Hsuehshan Range, Central Range and Coastal Range from west to east (Ho, 1986; Huang et al., 2012) (Fig. 2A). The Longitudinal Valley Fault is located between the Coastal Range and the Central Range, which are accretionary prism and volcanic arc respectively formed in the course of the eastward subduction of South China Sea (Fig. 2A). The Coastal Plain, the Western Foothills and the Hsuehshan Range are composed of deformed and uplifted passive continental margin sedimentary rocks including alternation of sandstones and shales with minor limestone and tuff lenses.

The Western Foothills, separated by Chuchih thrust fault with Hsuehshan Range, is composed of thick paralic sequences ranging from Oligocene to Pliocene in age and Eocene fluvial to swamp facies rocks. These strata can also be grouped into Eocene syn-rift sequences, Oligocene to upper Miocene post-rift sequences and Pliocene to Pleistocene foreland sequences (Fig. 3). In northern Western Foothills, the continuous stratigraphy ranging from Oligocene to upper Miocene is best exposed in the coastal sections near Keelung (Ho et al., 1964; Teng et al., 1991) (Fig. 3). These strata, from bottom to top, are Oligocene Wuchishan Formation, Lower Miocene Mushan, Taliao, Shihti Formations, Middle Miocene Nankang Formation and Upper Miocene Nanchuang, Kueizhulin Formations (Fig. 3). In central Western Foothills, the detailed biostratigraphic studies in Kuohsing Peikang River Section (Fig. 2D) in Nantou County show that the lithology and sequences in central Taiwan are correlative with the stratotype in northern Taiwan (Huang and Ting, 1979; Huang, 1986) (Fig. 3). Within the

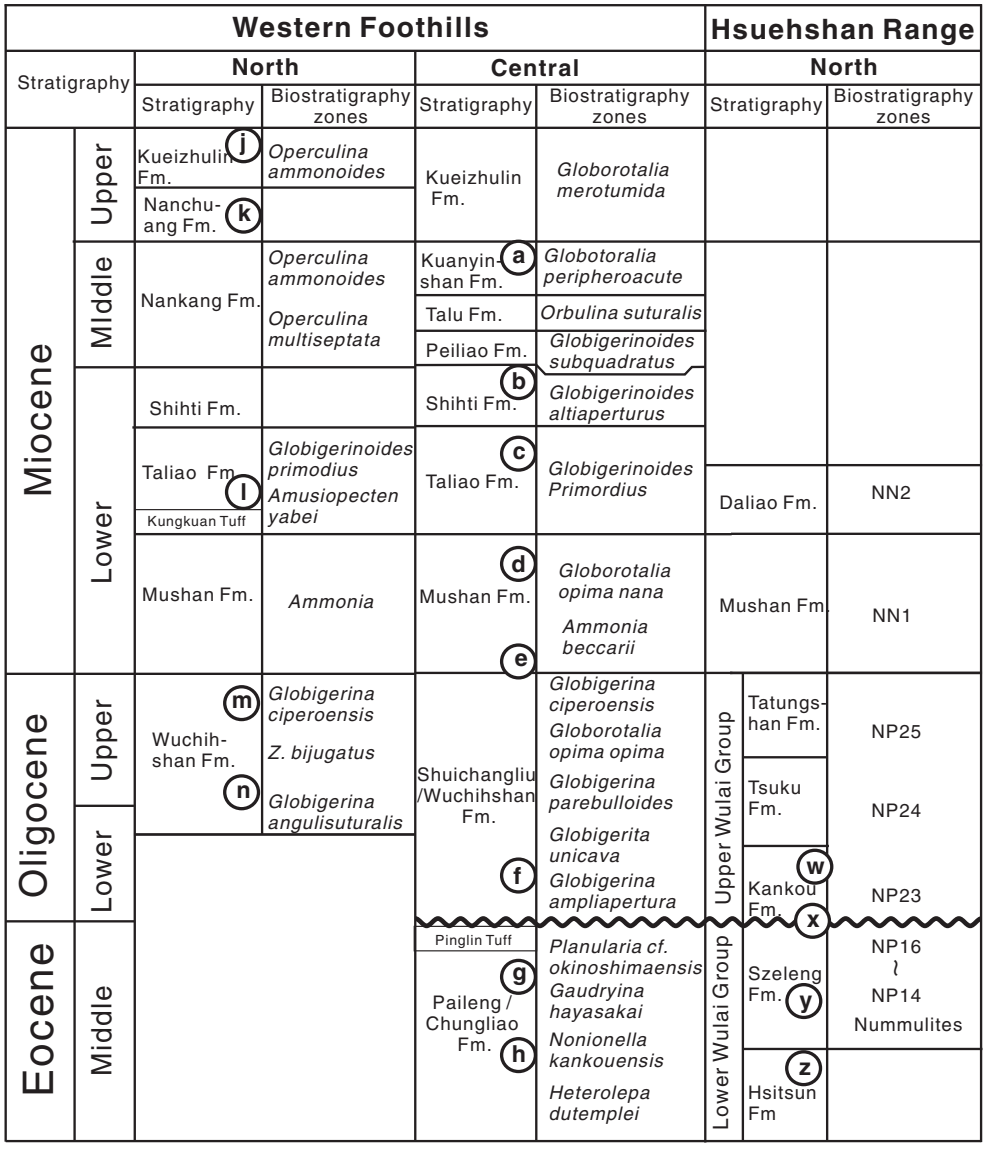

Fig. 3. The Cenozoic stratigraphic of north, south Western Foothills and Hsuehshan Range. The biostratigraphic data is summarized from Huang and Cheng (1983), Huang (1986), Huang and Ting (1979), Chi (1979), Teng et al. (1991), Ho (1969), Huang et al. (1979) and references therein. The lowercases in the circles are correspondent to those in Fig. 6.

Tsukeng Anticline (Fig. 2A, C), the indigenously buried *Discocyclina dispansa* foraminifera was identified together with interbedded tuff (Pinglin Tuff) that was dated as ca.39 Ma (Huang et al., 2013; Lan et al., 2014), suggesting that the sedimentary history of the Western Foothills is much longer than previously recognized (Ho et al., 1956; Ho, 1961).

The Hsuehshan Range is located at the east of Western Foothills and the west of Central Range (Fig. 2A). It is dominated by thick argillites, sandstones and slates ranging from Eocene to Miocene (Fig. 3). The Eocene Hsitsan Formation to Upper Oligocene Tatungshan Formation is well exposed along the Peishichi Section in northern Taiwan (Fig. 3). The strata in northern Hsuehshan Range, from bottom to top, are Eocene Hsitsun and Szeleng Formations (Lower Wulai Group) in the lower part, Oligocene Kankou, Tsuku and Tatungshan Formations (Upper Wulai Group) and Lower Miocene Mushan and Taliao Formations (Fig. 3). There has been a general consensus in earlier studies that the Oligocene Upper Wulai Group which consist of argillites and siltstones with abundant shallow marine fossils (Chang, 1962; Huang, 1977) is conformably overlying the Lower Wulai Group (Chang, 1975), which is predominated by conglomerates, sandstones and siltstones with rich plant remains, indicating braided river-lacustrine depositional environment. The recent study on stratigraphy by Huang et al. (2012) demonstrates that the depositional age of the Szeleng Formation is Middle Eocene and that an unconformity occurs between the Upper and Lower Wulai Group (Fig. 3).

3. Sampling and analytical methods

The sandstones collected from the Western Foothills and Hsuehshan Range in Taiwan (Figs. 2 and 3) were crushed to 60 mesh. Zircon grains were separated by washing, electromagnetic and heavy liquid techniques followed by handpicking under a binocular. Around 300 zircon grains were mounted randomly in epoxy resin and polished to expose the core of each grain. The analytical spots were chosen based on careful examination of cathodoluminescence (CL) images for internal morphology prior to analysis. The CL images were acquired with a Mono CL3 + (Gatan, USA) attached to a scanning electron Microscope (Quanta 400 FEI) in the State Key Laboratory of Continental Dynamics, Northwest University, Xi'an. The sample surface was cleaned with ethanol to eliminate possible contamination before analysis. In order to reduce the probability of error (Dodson et al., 1988; Zhang et al., 2012), we analyzed at least 120 zircon grains from each sample.

3.1. U-Pb dating

Zircon U-Pb dating was performed by laser-ablation-inductively coupled plasma- mass spectrometry (LA-ICP-MS) at the Guangzhou Institute of Geochemistry. The RESOLUTION M-50 laser-ablation system equipped with a 193 nm excimer ArF laser-ablation system was used, which is connected with an Agilent7500a ICP-MS. Helium was used as the carrier gas to enhance the transport efficiency of the ablated material. The helium carrier gas inside the ablation cell was mixed with argon gas before entering the ICP to maintain stable and optimum excitation conditions. The analyses were conducted with a beam diameter of 32 μm with analysis time including ~30 s background measurement with laser off and a 60s measurement of peak intensity. Zircon Temora (the U-Pb age is 416.75 ± 0.24 Ma; Black et al., 2003) was used as the standard, and the standard silicate glass NIST 610 was used to optimize the instrument. The age of Plešovice zircon as used as unknown is 338 ± 5 Ma, which is close to the recommended age of 337 ± 0.4 Ma (Sláma et al., 2008). Offline selection and integration of background and analytic signals and time-drift correction and quantitative calibration for trace element analyses and U-Pb dating were performed using software ICPMSDataCal (Liu et al., 2009; Y. Liu et al., 2010). U, Th and Pb concentrations were calibrated using ^{29}Si as an internal standard and NIST 610 as reference material. The age calculation and age spectra plots were made using ISOPLOT (version 3.0) (Ludwig, 2003). Counting statistics shows that $^{206}Pb/^{238}U$ ages are generally more precise for younger zircons, whereas $^{206}Pb/^{207}Pb$ ages are more precise for older ones, so we choose to use $^{206}Pb/^{238}U$ ages for ≤1000 Ma zircons and $^{207}Pb/^{206}Pb$ ages for those above 1000 Ma (Xu et al., 2007; Duan et al., 2011).

3.2. Lu-Hf isotope analysis

In situ zircon Hf isotopic analyses were conducted at the State Key Laboratory of Continental Dynamics, Northwest University, Xi'an using a Nu Plasma HR MC-ICP-MS (Nu instruments Ltd., UK), coupled to a GeoLas 2005 excimer ArF Laser-ablation system. The analytical technique followed those described by Yuan et al. (2008). During analyses, the Harvard zircon 91500 standard was used as a standard; the $^{176}Hf/^{177}Hf$ ratio obtained was 0.282299 ± 9, similar to the recommended $^{176}Hf/^{177}Hf$ ratio of 0.282306 ± 10 measured using the solution method (Woodhead et al., 2004). The ^{176}Lu decay constant of 1.865×10^{-11} yr^{-1} reported by Scherer et al. (2001) was adopted in this study. The chondritic values of $^{176}Hf/^{177}Hf$ (0.282772) and $^{176}Lu/^{177}Hf$ (0.0332) reported by Blichert-Toft and Albarède (1997) were used in calculations.

4. Analytical results

Zircons extracted from the samples are light yellow to colorless. Most of the zircons show oscillatory zoning (Fig. 4), indicating typical igneous origin, but the others show irregular internal structure of metamorphic zircons. The majority of the zircons have Th/U > 0.3, suggesting igneous origin, and few grains show Th/U < 0.1 corresponding to metamorphic origin (Fig. 5) (Corfu et al., 2003; Hoskin and Schaltegger, 2003).

4.1. Zircon U-Pb geochronology

In situ U-Pb ages of the zircon grains listed in Appendix A. The age distribution of zircon grains from the sandstones in central Western Foothills, northern Western Foothills and Hsuehshan Range, respectively, are presented in Fig. 6.

4.1.1. Central Western Foothills in Taiwan

The age distribution of zircon grains from sandstones in the Central Western Foothills (Fig. 2C and D) can apparently be divided into two groups: the Eocene to Oligocene group (within purple dotted line in Fig. 6) and the Miocene group (within blue dotted line in Fig. 6) (Fig. 6a–h). The U-Pb age of two Eocene samples (PL-11, SZ-738) from Chungliao Formation in Tsukeng Anticline Section and Paileng Formations in Kuohsing Peikangchi Section, respectively, indicates that over 65% zircons are younger than 500 Ma, with main age peaks of 115 Ma, 140 Ma, 240 and 431 Ma for PL11 and 80 Ma, 163 Ma, 264 Ma and 430 Ma for SZ-738 (Fig. 6g, h). The remaining zircon grains show scattered age distribution from 700 Ma to 2500 Ma with no major peak. The Oligocene Wuchihshan (PL-6) sample has over 70% young zircons (<500 Ma) with 96 Ma peak and shows scattered distribution for the older zircon grains (Fig. 6f).

The Miocene samples have very distinctive U-Pb age pattern of detrital zircon grains. The percentage of zircon grains that is younger than 500 Ma is markedly lower (Fig. 6a–e). For example, the young zircons (<500 Ma) in Mushan, Taliao and Shihti Formations account for less than 30% except for those in the Kuanyinshan Formation with 36% and show major age clusters of 110–130 Ma, 180–250 Ma and 350–450 Ma (Fig. 6b–e). There is a sharp increase in the old zircon population during Miocene with major peaks at 740–810 Ma for the 650–1000 Ma group, at 1720–1890 Ma and 2440–2520 Ma for the 1500–2800 Ma cluster. Zircons with ages over 3000 Ma are scarce (Fig. 6a–h).

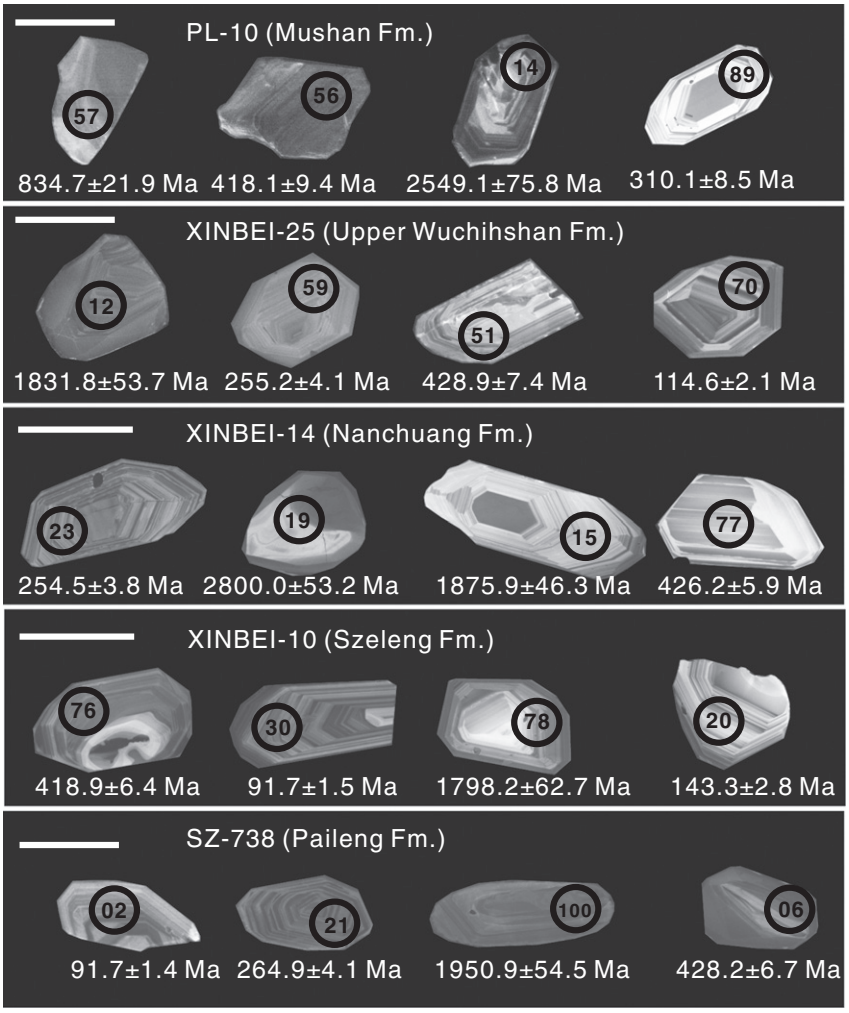

Fig. 4. Representative cathodoluminescence (CL) images of detrital zircon grains from Cenozoic sedimentary rocks. Scale bar = 50 μm. Some of the grains (SZ-738-100; XINBEI-14-19) show rounded morphology, suggesting reworking or a longer transport distance from their source.

4.1.2. Northern Western Foothills in Taiwan

The U-Pb zircon age spectra from the Northern Western Foothills in Taiwan (Fig. 2B) are very similar with the central ones (Fig. 6a–n). The zircon grains with ages below 500 Ma are dominant (>50%) in the two Oligocene samples (XINBEI-22, XINBEI-25) with age clusters of 90–180 Ma, 200–270 Ma and 370–450 Ma, including peaks at 137 Ma, 169 Ma, 223 Ma and 407 Ma. The remaining zircon grains yield scattered age distribution from 700 Ma to 2600 Ma without any obvious peaks (Fig. 6m, n). The Miocene sandstones, however, show markedly different age pattern as compared with the Oligocene ones in having over 66% old zircons (>600 Ma), with major age peak at around 800 Ma and a wide age distribution between 1500–2100 Ma and 2200–2800 Ma (Fig. 6j–l).

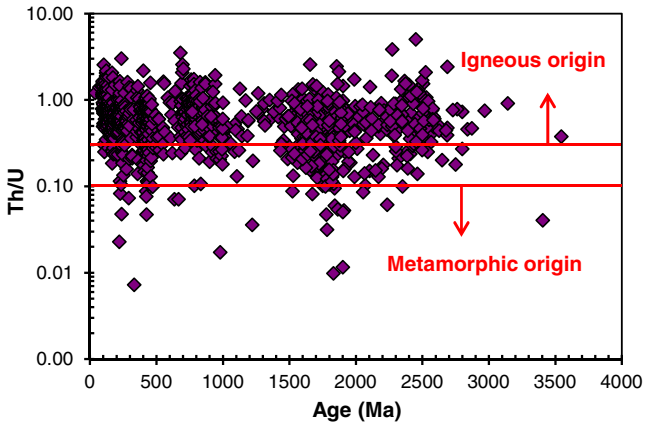

Fig. 5. The Th/U ratio of zircon grains with different ages. The zircon grains with Th/U >0.3 or <0.1 suggest igneous or metamorphic origin respectively (Corfu et al., 2003; Hoskin and Schaltegger, 2003). The data suggest that most of the zircon grains from Taiwan are of igneous origin, and therefore, their U-Pb ages reflect the time of crystallization.

4.1.3. Hsuehshan Range in Taiwan

Samples collected from Hsuehshan Range are dominated by young zircon grains (<500 Ma) with an exception of those in sample XINBEI-12, where they account for only 38% (Fig. 6w–z). The four sandstones from Hsuehshan Range show similar age pattern with clusters of 90–180 Ma, 200–300 Ma and 380–450 Ma. The remaining zircon grains show wide and discontinuous ages from 700 to 2700 Ma with no significant age peaks except for the zircons in sample XC11-1 which display minor peaks at 715 Ma and 926 Ma (Fig. 6z).

4.2. Hf isotopic characteristics of detrital zircon grains in Taiwan

The Hf isotopic results for 312 zircon grains from seven samples are shown in Appendix B and plotted in Fig. 7. The $\varepsilon Hf(t)$ values of detrital zircon grains from Taiwan exhibit a wide range from −63.8 to +14.8. The zircon grains from Eocene samples have negative $\varepsilon Hf(t)$ values

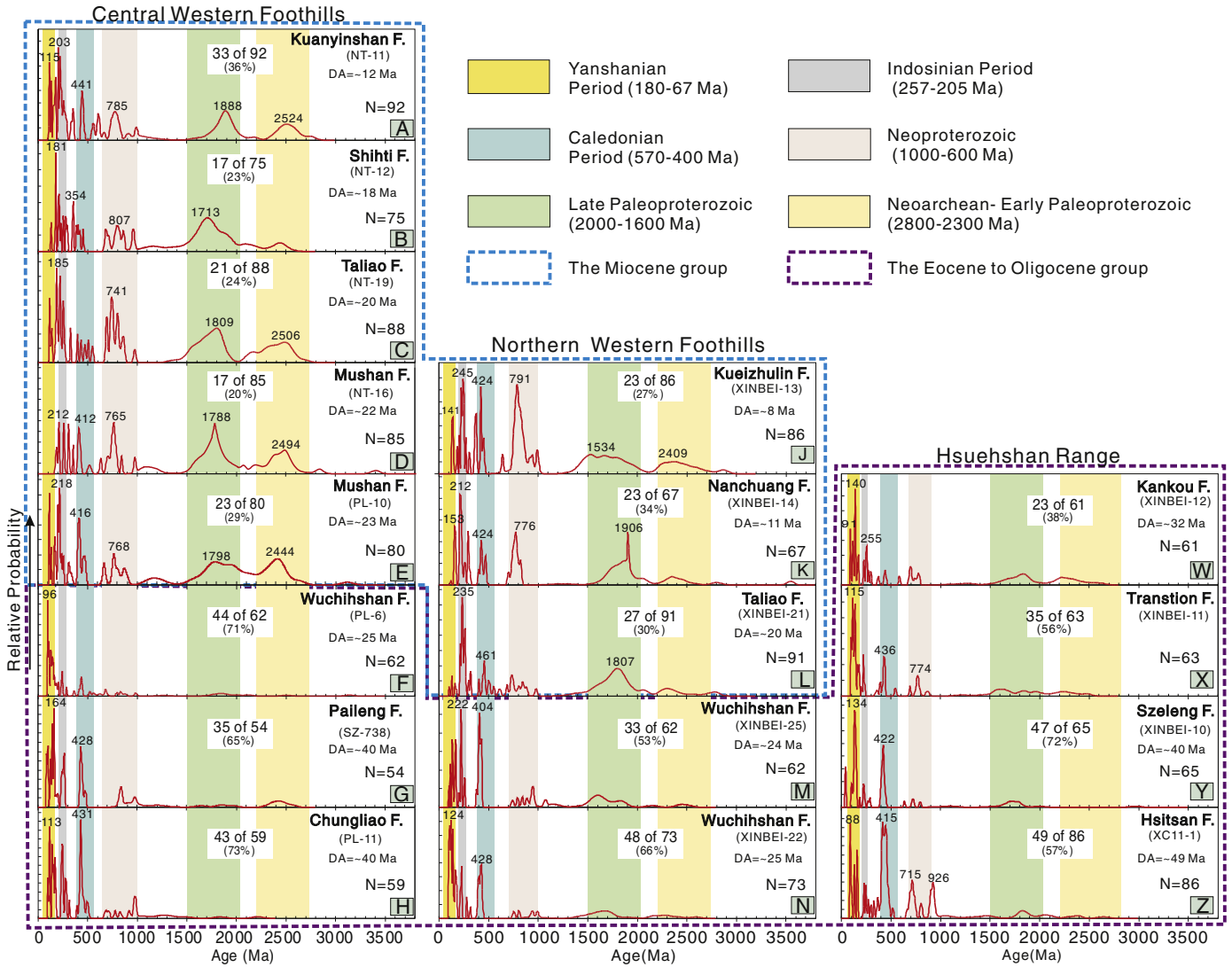

Fig. 6. The U-Pb age spectra of detrital zircons from Eocene to upper Miocene strata in Taiwan. a–h, j–n and w–z sandstone samples are from Central, northern Western Foothills and Hsuehshan Range, respectively. The percentage in white boxes represent the proportion of young zircon grains (<500 Ma) of the total. "DA" means depositional age.

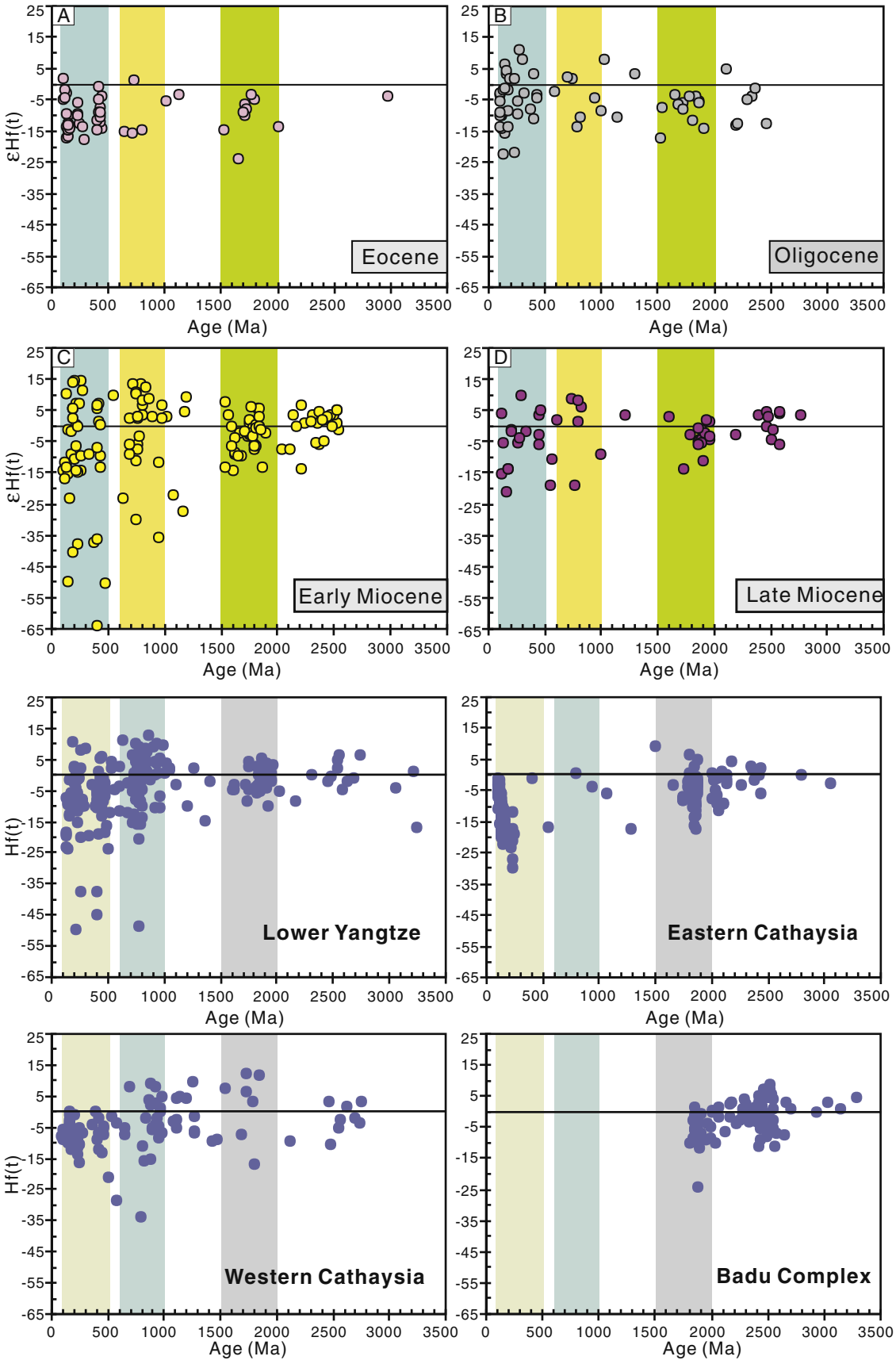

Fig. 7. The U-Pb age and εHf(t) values for detrital zircon grains extracted from Cenozoic stratigraphy in Taiwan.

(ranging from −24.1 to −0.9 and with an average of −9.9) except for two spots (+1.9, +1.6) (Appendix B, Fig. 7A). The majority of Phanerozoic zircons in Oligocene samples show εHf(t) values ranging between −15 and +5, and about 20% of zircon grains show positive values. The Precambrian zircon grains have εHf(t) values ranging from −17.2 to 7.8. The zircon grains with age of 1500–2000 Ma show negative εHf(t) values between −17.2 and −3.2 (Fig. 7B).

A marked change is observed in Early Miocene samples, where the young zircons with U-Pb ages below 500 Ma show more variable εHf(t) values ranging from −65 to +15. Most of the values fall between −16.8 and +14.8, and 37% of zircon grains display positive εHf(t) value (Fig. 7B). The Neoproterozoic zircon grains have a larger range than those with similar age in the Eocene and Oligocene samples. The zircons with age range of 1500–1900 Ma and 2100–2500 Ma possess εHf(t) values between −15 and +10, and almost symmetrically fall across the zero line (Fig. 7C). The zircon grains in Late Miocene samples seem to share Hf isotopic characteristics with those in Early Miocene samples, although the number of grains analyzed are limited (Fig. 7D).

5. Discussion

5.1. The provenance of Western Foothills and Hsuehshan Range

Although the paleo-current studies of strata in Western Foothills and Hsuehshan Range indicate west or northwest source region (Tan and Youh, 1978; Chou, 1988), Yokoyama et al. (2007) interpreted that the provenance of Hsuehshan Range is located within the drainage basin of the Pearl River and not the Western Foothills source from Korean Peninsula and paleo-Yangtze River, based on the detrital monazite age distribution of Eocene to Oligocene sandstones from Western Foothills and Hsuehshan Range.

Our age spectra of detrital zircon grains from Taiwan demonstrate that the Late-Middle Silurian (460–400 Ma), Early Triassic (260–210 Ma), Middle Jurassic to Early Cretaceous (180–120 Ma) and Early to Late Cretaceous (120–90 Ma) zircon grains are dominant in Eocene (Fig. 8B) to Oligocene (Fig. 8A) rocks from both Western Foothills and Hsuehshan Range. The Silurian zircon grains might have been derived from the Caledonian (570–400 Ma) granitoids in southeast China (Shu, 2006; R. Liu et al., 2010), which might be broadly related to the assembly of the Gondwana supercontinent (Rino et al., 2008; Duan et al., 2011). The Indosinian (257–205 Ma) and Yanshanian (180–67 Ma) granites in South China might have contributed the Mesozoic zircon grains in Taiwan. It can therefore be inferred that the Eocene to Oligocene sandstones from Hsuehshan Range and Western Foothills sourced from the same region. The reason that detrital monazite age distribution is quite different between Hsuehshan Range and Western Foothills (Yokoyama et al., 2007) is probably due to the limited detrital monazite grains in Hsuehshan Range samples and also because the age comparison was not conducted in the strata with the same depositional age.

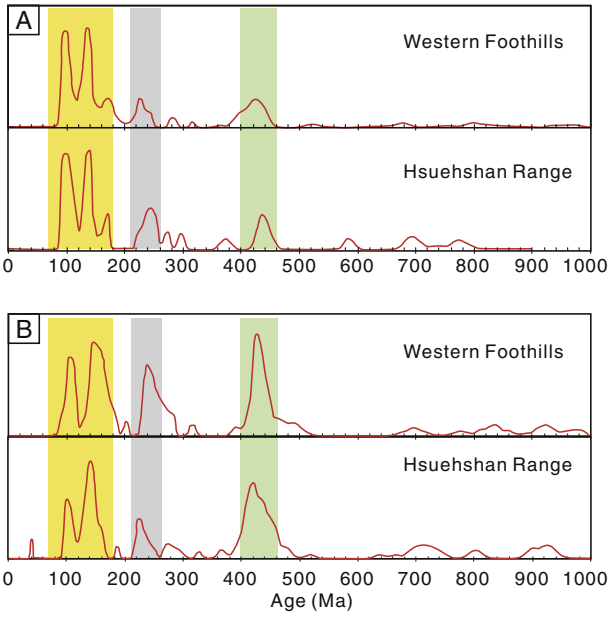

Fig. 8. Comparison of U-Pb age spectra for detrital zircon grains from Eocene (B) and Oligocene (A) samples in Western Foothills and Hsuehshan Range. The strata with the same age in Western Foothills and Hsuehshan Range show similar distribution of U-Pb age.

5.2. The evolution of sedimentary source of Cenozoic stratigraphy in Taiwan

The South China Craton has a complex tectonic evolution history and is composed of Yangtze Block to the northwest and Cathaysia Block to the southeast, separated by a series of major faults (Fig. 1). The Cathaysia Block has a Paleoproterozoic basement and the 1.9–1.7 Ga period is also regarded as an important period of crustal growth in the Cathaysia Block (Li, 1997; Yu et al., 2009; Li et al., 2012; Yu et al., 2012). The Yangtze Block has an older history than Cathaysia Block. The Neoproterozoic magmatic activities are considered to be important in the Yangtze Block and less significant in the Cathaysia Block, possibly related to the breakup of the Rodinia supercontinent (Wong et al., 2011; Li et al., 2012).

Abundant Neoproterozoic igneous rocks have been reported from the southeastern margin of the Yangtze Block (Li et al., 2008; Wang et al., 2010; Li et al., 2011) (Fig. 9). The detrital zircon grains of modern rivers in East Cathaysia Block show Mesozoic ages, with Yanshanian population dominating, and with no or less Neoproterozoic and Paleoproterozoic grains (Xu et al., 2007; Xu and Chen, 2010 and our unpublished data) despite the fact that Neoproterozoic igneous rocks are present in the Cathaysia Block (Li et al., 2005; Wan et al., 2007). This is possibly because most of these rocks are mafic in composition, with less or no zircon grains.

The comprehensive analysis of 312 Hf isotopic data and 1119 U-Pb age data of detrital zircon grains obtained from Eocene to Late Miocene sandstones in Taiwan in our study provide important insights into provenance evolution. The relative probability plots of the U-Pb zircon ages demonstrate that the Yanshanian period (180–67 Ma) zircon grains are dominant in Eocene and Oligocene rocks (Fig. 6). However, the Miocene sandstones show a different scenario where Indosinian period (257–205 Ma) zircon grains (Fig. 6) constitute the major population. The Permian to Cretaceous igneous rocks, which can be grouped into Indosinian periods and Yanshanian period, are widely distributed in the coastal region of South China. Although the petrogenesis of these rocks is disputed, a systematic variation younging from inland to coast region for the age of igneous rocks have been recognized (Li, 2000; Zhou and Li, 2000; Zhou et al., 2006; Li and Li, 2007) (Fig. 9). Thus, the change of provenance in Oligocene and lower Miocene strata might suggest that the source area migrated inland over time. Furthermore, the percentage of Precambrian zircon grains in Cenozoic rocks of Taiwan also shows a dramatic change. The Eocene and Oligocene sandstones rarely contain any Neoproterozoic (1000–600 Ma), late Paleoproterozoic (2000–1600 Ma) and Neoarchean–early Paleoproterozoic (2800–2300 Ma) zircon grains, in contrast to their abundance in the Miocene rocks (Fig. 6). One exception is that the Eocene Hsitsan Formation shows two minor Neoproterozoic peaks at 715 and 926 Ma (Fig. 6). Although the reason is unclear, the young zircons still dominate, which is consistent with the other Eocene and Oligocene Formations (Fig. 6).

The U-Pb age spectra of detrital zircon grains indicate that the source region of Oligocene to Eocene sandstones located coast of southeast China, and then migrated inland over time. The inland signals of zircon ages are clearly represented in Miocene sandstones. The source area of Miocene rocks may reach to southeast Yangtze Block as indicated by

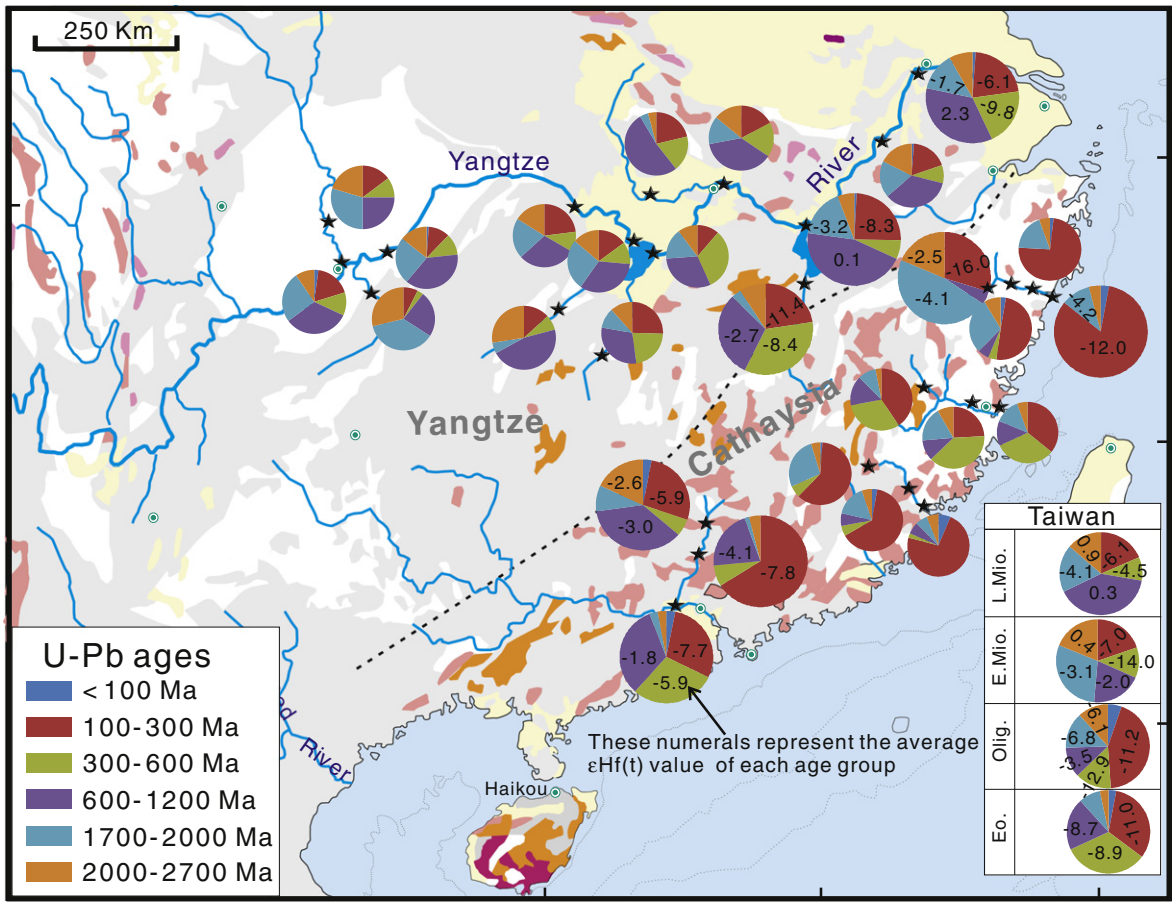

Fig. 9. Pie charts showing the range of zircon U-Pb ages for modern sands in rivers in South China and sedimentary rocks in Taiwan. The numerals in bigger pie charts refer to the average εHf(t) values of each age group.

the Neoproterozoic (1000–600), late Paleoproterozoic (2000–1600 Ma) and Neoarchean–early Paleoproterozoic (2800–2300 Ma) populations, which mainly distribute along the southeast margin of Yangtze Block (Li et al., 2008; Wang et al., 2010; Li et al., 2011) (Fig. 9).

We compiled the published εHf(t) data of detrital zircon grains from Lower Yangtze, eastern and western Cathaysia regions (Xu et al., 2007; He et al., 2013) in order to assess the detailed sedimentary source of Cenozoic rocks in Taiwan. The results show obvious disparities (Fig. 10). The Phanerozoic zircon grains with positive εHf(t) values are mainly distributed in the Lower Yangtze region (Fig. 10), although their percentage is limited. This is consistent with the previous study which suggested that the Yanshanian granitoids possess systematic Hf isotopic compositional variation across the Jiangshan–Shaoxing Fault (the boundary of Yangtze and Cathaysia Blocks) with the εHf(t) values falling between +7 and −7 in southeast Yangtze Block and between +1.9 and −13 in East Cathaysia (Wong et al., 2011). The majority of Phanerozoic zircon grains in the Lower Yangtze region have negative εHf(t) values (as low as ca. −50), suggesting derivation from magmas generated by recycling of crustal materials (He et al., 2013). Most of the εHf(t) values of zircon grains from Eastern Cathaysia show mostly negative values for the 1500–2000 Ma zircon grains, which is different from the data from further inland area of Western Cathaysia and Lower Yangtze region (Figs. 9 and 10). Although the 600–1000 Ma zircon grains in the Lower Yangtze area and Cathaysia Block show no significant differences in their εHf(t) values (+15 ~ −20) (Fig. 10), the zircon grains of this age are mainly distributed in Western Cathaysia and southeastern margin of the Yangtze Block (Li et al., 2011).

Our Hf isotopic data in this study show that almost all of the Phanerozoic and Paleoproterozoic zircon grains in Eocene sandstones have negative εHf(t) values (ranging from +1 to −18) (Fig. 7), which is comparable to the data from Eastern Cathaysia. The data suggest that the source region of the Eocene rocks located in the coast of southeast China at that time. The Oligocene sandstones shows transitional characteristic from Eocene to Early Miocene. The Phanerozoic zircon grains display large range in εHf(t) values (+10 ~ −22) in Oligocene sandstones, which is broadly similar with those of the zircons in Eocene rocks, although a comparison of the Hf isotope data show that part of the zircons, especially those with positive εHf(t) values were possibly derived from the Lower Yangtze region. The data suggest that the provenance of Oligocene strata is still dominated by the coastal area, with little contribution from Lower Yangtze or Western Cathaysia during late Oligocene (Figs. 7 and 10). Similar to the U-Pb age spectra, the Hf isotopes of detrital zircons also show a major change in the Miocene sandstones, which include many grains with Lower Yangtze and Western Cathaysia characteristics that the εHf(t) values display large variation for both Phanerozoic and Paleoproterozoic zircon grains (Figs. 7 and 10). Thus, the variation trends of U-Pb ages and Hf isotope of detrital zircon grains from Cenozoic sandstones in Taiwan indicate that their provenance migrated inland greatly during Late Oligocene and Early Miocene, which is consistent with the variation of the Nd isotope values reported from mudstones (Lan et al., 2014). The source region of Neogene formations might have already reached up to the Lower Yangtze area or West Cathaysia, although it is more likely derived from the Yangtze Craton.

5.3. The tectonic controls on evolution of drainage system and landscape in East Tibet

We consider the change in provenance as a passive signal of an evolution of landscapes and river systems. The U-Pb age spectra of detrital

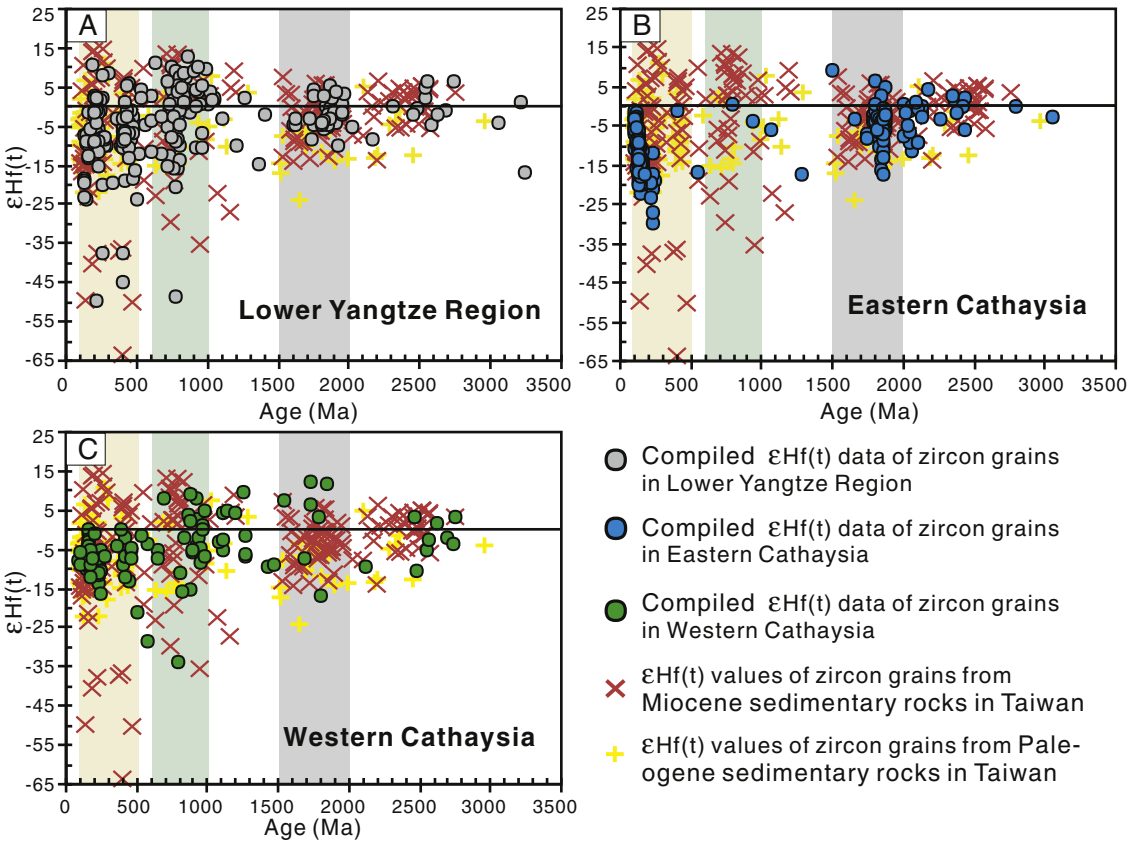

Fig. 10. The published U-Pb age and εHf(*t*) values of zircon grains in (A): Low Yangtze Region (He et al., 2014); (B and C): East and West Cathaysia Block (Xu et al., 2007).

zircon grains in Cenozoic strata in Taiwan can apparently be divided into two groups: the Eocene–Oligocene group that is comparable to the modern sediments collected from river mouth in coast of southeast China, especially Minjiang River, and the Miocene group that is analogous to those in Yangtze delta and Lower Yangtze region (Fig. 11). This transition trend may indicate that the Minjiang River systems or rivers draining like the Minjiang that drain similar sources supplied the main sediments for Paleogene strata in Taiwan.

The change of sedimentary source for Miocene stratigraphy may imply two potential possibilities. One is that the Yangtze River delivered major sediments to the original region of uplifted Taiwan starting from Early Miocene. Although the long distance transport is difficult to

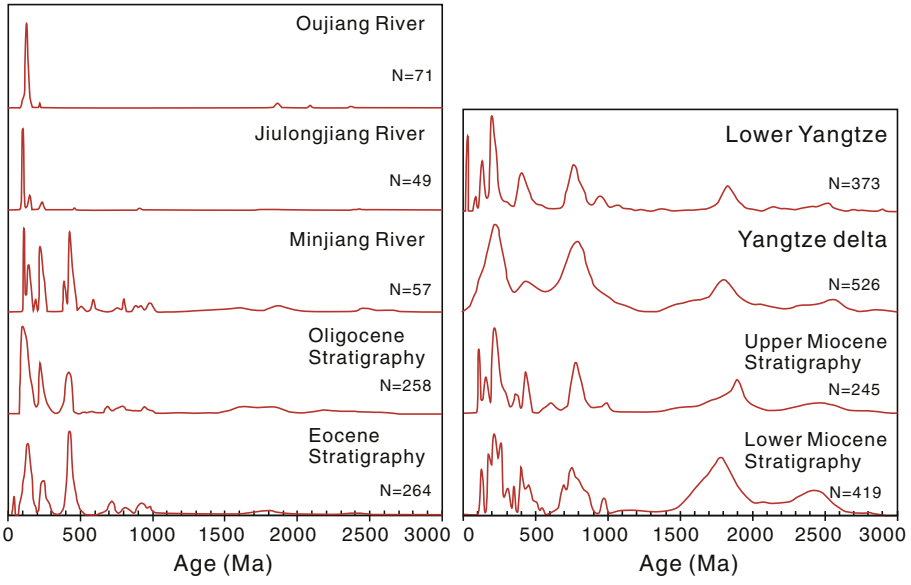

Fig. 11. Left: Comparison of U-Pb age spectra of detrital zircon grains from Eocene–Oligocene strata in Taiwan with those from modern river mouth sediments in southeast China: Minjiang River, Jiulongjiang River (our unpublished data) and Oujiang River (Xu et al., 2007). These strata have similar age distribution with Minjiang River, which run through East Cathaysia Block. Right: the U-Pb age distribution of detrital zircon grains from Miocene strata in Taiwan and modern sediments in Lower Yangtze and Yangtze delta (Zheng et al., 2013; He et al., 2014).

explain at present, some evidence suggests that the paleogeographic framework of East China Sea is different with what it is today (Zhang, 2008; Clift et al., 2013a,b). However, some workers consider that the paleo-Yangtze river mouth was in the Subei Basin in the north (Zheng et al., 2013). Therefore, the more likely scenario is that the Minjiang River could have been larger than what it is now in Early Miocene and reached up to the boundary of the Yangtze and Cathaysia Blocks. The headwaters of this river were subsequently captured by the Yangtze River systems at some time after Late Miocene.

During the seafloor spreading of marginal sea, the northern continental margin of South China Sea had gone through extensive thermal subsidence stage starting from late Oligocene (Zhou et al., 1995). The erosion rate of northern margin of the South China Sea apparently decreased and the westward propagation of the paleo-Pearl River drainage since late Oligocene (Pang et al., 2006; Yan et al., 2009a,b). Together with the evolution of drainage systems recorded by the Cenozoic sediments in Taiwan in this study, it is possible that the opening of marginal sea, such as the South China Sea, exerted a major influence on the evolution of topography and drainage system in southeast China. This can also be proved from the diachronism features of breakup unconformity and transition of provenance in basins in northern margin of South China Sea (Lan et al., 2014). The transition time of provenance in rifted basins in northern margins of South China Sea, the same with breakup unconformity, shows obvious diachronism. For example, the transition time of provenance in Taiwan is 31–25 Ma, the ODP site 1148 and Pearl River Mouth Basin is 27–23 Ma and the Yinggehai-Qiongdongnan Basin is ~13 Ma. The diachronism of breakup unconformity and transition time of provenance implied that the opening of SCS had great influence on the evolution of provenance, topography and river systems in southeast China.

Although a large amount of data suggest the multi-stage growth during Cenozoic (Harrison et al., 1992; Zhong and Ding, 1996; Tapponnier et al., 2001), thermochronology study shows that the Eastern Tibet Plateau had undergone rapid uplift starting in Late Oligocene (Wang et al., 2012). Previous studies have shown that the middle Yangtze River flowed westward in to paleo-Red River (Clift et al., 2006; Yan et al., 2012). The river systems in East Tibet have gone through major adjustment during late Oligocene to early Miocene (Clift et al., 2006; Zheng et al., 2013; Robinson et al., 2014). The Nd isotopic composition of sediments from the Hanoi Basin and zircon age spectra from the downstream of Yangtze River show the establishment of modern drainage systems in East Tibet by ca.24 Ma (Clift et al., 2006; Zheng et al., 2013). This is in conformity with the change in time of topography and drainage systems in southeast China as recorded in this study. Therefore, the establishment of present topography and drainage system in East Tibet was mainly controlled by the tectonic events of Eastern Tibet uplift and the opening of marginal sea, as well as the evolution of topography and drainage systems in southeast China, which were mainly controlled by the opening of marginal sea.

6. Conclusion

This study employed U-Pb age and Hf isotope of detrital zircon grains in probing the provenance evolution as a passive marker to landscapes and river systems. The zircon U-Pb data show that the Hsuehshan Range and Western Foothills share the same sedimentary source. The evolution history of provenance of Cenozoic strata in Taiwan is restored in this study. Our U-Pb and εHf data demonstrate that zircon grains in the Eocene–Oligocene sedimentary rocks in Taiwan mainly originated in Phanerozoic igneous rocks along the coastal area of southeast China. The provenance gradually migrated inland and the source region of Miocene strata probably migrated to Lower Yangtze region, which was accompanied by inland erosion of river system in southeast China. The Minjiang River might have been larger than what it is now with its upper reaches extending to the Lower Yangtze region. The river was then captured by the tributary of Yangtze River system at some time after late Miocene. The provenance reconstruction emphasizes the role that opening of marginal sea plays in the evolution of drainage systems and landscapes in southeast China during late Oligocene to early Miocene.

Supplementary data to this article can be found online at http://dx.doi.org/10.1016/j.gr.2015.07.008.

Acknowledgments

This work was financially co-supported by the National Natural Science Foundation of China (grant nos. 41176041, 41476036 and 91128211) and the Key Laboratory of Marine Mineral Resources, Ministry of Land and Resources (grant nos. KLMMR-2013-B-04 and GZH201200601). This is contribution (GIGRC-10-01) IS-2122 from GIGCAS.

References

Black, L.P., Kamo, S.L., Allen, C.M., Aleinikoff, J.N., Davis, D.W., Korsch, R.J., Foudoulis, C., 2003. TEMORA 1: a new zircon standard for Phanerozoic U-Pb geochronology. Chemical Geology 200, 155–170.
Blichert-Toft, J., Albarède, F., 1997. The Lu-Hf isotope geochemistry of chondrites and the evolution of the mantle-crust system. Earth and Planetary Science Letters 148, 243–258.
Briais, A., Patriat, P., Tapponnier, P., 1993. Updated interpretation of magnetic anomalies and seafloor spreading stages in the South China Sea: implications for the Tertiary tectonics of Southeast Asia. Journal of Geophysical Research: Solid Earth (1978–2012) 98, 6299–6328.
Burchfiel, B., Zhiliang, C., Yupinc, L., Royden, L., 1995. Tectonics of the Longmen Shan and adjacent regions, central China. International Geology Review 37, 661–735.
Chang, L.S., 1962. Some planktonic foraminifera from the Suo and Urai Groups of Taiwan and their stratigraphic significance. Proceedings of the Geological Society of China 5, 47–64.
Chang, L., 1975. Tertiary biostratigraphy of Taiwan. Geology and Paleontology of Southeast Asia 15, 337–361.
Chen, J.F., Jahn, B.M., 1998. Crustal evolution of southeastern China: Nd and Sr isotopic evidence. Tectonophysics 284, 101–133.
Chi, W.R., 1979. Calcareous nannoplankton biostratigraphy of the Nantou area, central Taiwan. Petroleum Geology of Taiwan 16, 131–165.
Chou, J.T., 1977. Sedimentology and paleogeography of the Pleistocene Toukoshan Formation in western Taiwan. Petroleum Geology of Taiwan 14, 25–36.
Chou, J.T., 1980. Stratigraphy and sedimentology of the Miocene in western Taiwan. Petroleum Geology of Taiwan 17, 33–52.
Chou, J.T., 1988. Eocene formations in Taiwan. Petroleum Geology of Taiwan 24, 51–59.
Clark, M.K., Schoenbohm, L.M., Royden, L.H., Whipple, K.X., Burchfiel, B.C., Zhang, X., Tang, W., Wang, E., Chen, L., 2004. Surface uplift, tectonics, and erosion of eastern Tibet from large-scale drainage patterns. Tectonics 23, TC1006. http://dx.doi.org/10.1029/2002TC001402.
Clark, M.K., House, M.A., Royden, L.H., Whipple, K.X., Burchfiel, B.C., Zhang, X., Tang, W., 2005. Late Cenozoic uplift of southeastern Tibet. Geology 33, 525.
Clift, P., Lee, J.I., Clark, M.K., Blusztajn, J., 2002. Erosional response of South China to arc rifting and monsoonal strengthening: a record from the South China Sea. Marine Geology 184, 207–226.
Clift, P.D., Blusztajn, J., Anh Duc, N., 2006. Large-scale drainage capture and surface uplift in eastern Tibet–SW China before 24 Ma inferred from sediments of the Hanoi Basin, Vietnam. Geophysical Research Letters 33. http://dx.doi.org/10.1029/2006GL027772.
Clift, P.D., Carter, A., Nicholson, U., Masago, H., 2013a. Evolving Sediment Flux to the Nankai Trough; influence of the Yangtze River? Geophysical Research Abstracts 15.
Clift, P.D., Carter, A., Nicholson, U., Masago, H., 2013b. Zircon and apatite thermochronology of the Nankai Trough accretionary prism and trench, Japan: sediment transport in an active and collisional margin setting. Tectonics 32, 377–395.
Corfu, F., Hanchar, J.M., Hoskin, P.W., Kinny, P., 2003. Atlas of zircon textures. Reviews in Mineralogy and Geochemistry 53, 469–500.
Dodson, M.H., Compston, W., Williams, I.S., Wilson, J.F., 1988. A search for ancient detrital zircons in Zimbabwean sediments. Journal of the Geological Society 145, 977–983.
Duan, L., Meng, Q.-R., Zhang, C.-L., Liu, X.-M., 2011. Tracing the position of the South China block in Gondwana: U-Pb ages and Hf isotopes of Devonian detrital zircons. Gondwana Research 19, 141–149.
Fielding, E.J., 1996. Tibet uplift and erosion. Tectonophysics 260, 55–84.
Gaudette, H.E., Vitrac-Michard, A., Allegre, C.J., 1981. North American Precambrian history recorded in a single sample: high-resolution UPb systematics of the Potsdam sandstone detrital zircons, New York State. Earth and Planetary Science Letters 54, 248–260.
Harrison, T.M., Copeland, P., Kidd, W.S.F., Yin, A., 1992. Raising Tibet. Science 255, 1663–1670.
He, M., Zheng, H., Clift, P.D., 2013. Zircon U-Pb geochronology and Hf isotope data from the Yangtze River sands: implications for major magmatic events and crustal evolution in Central China. Chemical Geology 360–361, 186–203.
He, M., Zheng, H., Bookhagen, B., Clift, P.D., 2014. Controls on erosion intensity in the Yangtze River basin tracked by U-Pb detrital zircon dating. Earth Science Reviews 136, 121–140.

Ho, C.S., 1961. Correlation of the Takeng Formation and some related stratigraphic principles. Proceedings of the Geological Society of China 4, 61–71.
Ho, C.S., 1969. Stratigraphy of the Kungkuan Tuff in northern Taiwan. Bulletin of the Geological Survey of Taiwan 20, 41–62.
Ho, C.S., 1986. A Synthesis of the Geologic Evolution of Taiwan. Tectonophysics 125, 1–16.
Ho, C.S., Tsan, S.F., Tan, L.P., 1956. Geology and coal deposit of the Chichitashan area, Nantou, Taiwan. Bulletin of the Geological Survey of Taiwan 9, 1–64.
Ho, C.S., Hsu, M.Y., Jen, L.S., Fong, G.S., 1964. Geology and coal resources of the northern coastal area of Taiwan. Bulletin of the Geological Survey of Taiwan 15, 1–23.
Hoskin, P.W., Schaltegger, U., 2003. The composition of zircon and igneous and metamorphic petrogenesis. Reviews in Mineralogy and Geochemistry 53, 27–62.
Huang, T.C., 1977. Calcareous nannoplankton stratigraphy of the upper Wulai Group (Oligocene) in Northern Taiwan. Petroleum Geology of Taiwan 14, 147–179.
Huang, C.Y., 1986. Oligocene and Miocene stratigraphy of the Kuohsing area, central Taiwan. Acta Geologica Taiwanica 281–318.
Huang, C., Cheng, Y., 1983. Oligocene and Miocene planktic foraminiferal biostratigraphy of northern Taiwan. Proceedings of the Geological Society of China 26, 21–56.
Huang, T.C., Ting, J.S., 1979. Calcareous nannofossils succession from the Oligo-Miocene Peikangchi section and revised stratigraphic correlation between northern and central Taiwan. Proceedings of the Geological Society of China 22, 105–120.
Huang, C., Cheng, Y., Huang, T., 1979. Preliminary biostratigraphic study of the Nankang Formation in the Shuinantung section, northern Taiwan. Ti-Chih (Geology) 2, 1–11.
Huang, C.Y., Wu, W.-Y., Chang, C.-P., Tsao, S., Yuan, P.B., Lin, C.-W., Xia, K.-Y., 1997. Tectonic evolution of accretionary prism in the arc-continent collision terrane of Taiwan. Tectonophysics 281, 31–51.
Huang, C.Y., Yuan, P.B., Lin, C.-W., Wang, T.K., Chang, C.P., 2000. Geodynamic processes of Taiwan arc-continent collision and comparison with analogs in Timor, Papua New Guinea, Urals and Corsica. Tectonophysics 325, 1–21.
Huang, C.Y., Yen, Y., Zhao, Q., Lin, C.-T., 2012. Cenozoic stratigraphy of Taiwan: window into rifting, stratigraphy and paleoceanography of South China Sea. Chinese Science Bulletin 57, 3130–3149.
Huang, C.Y., Yen, Y., Liew, P.M., He, D.J., Chi, W.R., Wu, M.S., Zhao, M., 2013. Significance of indigenous Eocene larger foraminifera *Discocyclina dispansa* in Western Foothills, Central Taiwan: a Paleogene marine rift basin in Chinese continental margin. Journal of Asian Earth Sciences 62, 425–437.
Jia, J.T., Zheng, H.B., Huang, X.T., Wu, F.Y., Yang, S.Y., Wang, K., He, M.Y., 2010. Detrital zircon U-Pb ages of Late Cenozoic sediments from the Yangtze delta: implication for the evolution of the Yangtze River. Chinese Science Bulletin 55, 1520–1528.
Lan, Q., Yan, Y., Huang, C.Y., Clift, P.D., Li, X., Chen, W., Zhang, X., Yu, M., 2014. Tectonics, topography, and river system transition in East Tibet: insights from the sedimentary record in Taiwan. Geochemistry, Geophysics, Geosystems 15. http://dx.doi.org/10.1002/2014GC005310.
Li, X., 1997. Timing of the Cathaysia Block formation: constraints from SHRIMP U-Pb zircon geochronology. Episodes 20, 188–192.
Li, X.H., 2000. Cretaceous magmatism and lithospheric extension in Southeast China. Journal of Asian Earth Sciences 18, 293–305.
Li, J.J., Fang, X.M., 1999. Uplift of the Tibetan Plateau and environmental changes. Chinese Science Bulletin 44, 2117–2124.
Li, Z.X., Li, X.-H., 2007. Formation of the 1300-km-wide intracontinental orogen and postorogenic magmatic province in Mesozoic South China: a flat-slab subduction model. Geology 35, 179.
Li, J.J., Xie, S.Y., Kuang, M.S., 2001. Geomorphic evolution of the Yangtze Gorges and the time of their formation. Geomorphology 41, 125–135.
Li, X.H., Wei, G., Shao, L., Liu, Y., Liang, X., Jian, Z., Sun, M., Wang, P., 2003. Geochemical and Nd isotopic variations in sediments of the South China Sea: a response to Cenozoic tectonism in SE Asia. Earth and Planetary Science Letters 211, 207–220.
Li, W.X., Li, X.-H., Li, Z.-X., 2005. Neoproterozoic bimodal magmatism in the Cathaysia Block of South China and its tectonic significance. Precambrian Research 136, 51–66.
Li, W.X., Li, X.-H., Li, Z.-X., 2008. Middle Neoproterozoic syn-rifting volcanic rocks in Guangfeng, South China: petrogenesis and tectonic significance. Geological Magazine 145, 475–489.
Li, W.X., Li, X.H., Li, Z.X., 2011. Ca. 850 Ma bimodal volcanic rocks in northeastern Jiangxi Province, South China: initial extension during the breakup of Rodinia? American Journal of Science 310, 951–980.
Li, X.H., Li, W.-x., He, B., 2012. Building of the South China Block and its relevance to assembly and breakup of Rodinia supercontinent: observations, interpretations and tests (In Chinese with English abstract). Bulletin of Mineralogy, Petrology and Geochemistry 31, 543–559.
Lin, A.T., Watts, A.B., Hesselbo, S.P., 2003. Cenozoic stratigraphy and subsidence history of the South China Sea margin in the Taiwan region. Basin Research 15, 453–478.
Liu, Y., Gao, S., Hu, Z., Gao, C., Zong, K., Wang, D., 2009. Continental and oceanic crust recycling-induced melt–peridotite interactions in the Trans-North China Orogen: U-Pb dating, Hf isotopes and trace elements in zircons from mantle xenoliths. Journal of Petrology 51, 537–571.
Liu, R., Zhou, H., Zhang, L., Zhong, Z., Zeng, W., Xiang, H., Jin, S., Lu, X., Li, C., 2010a. Zircon U-Pb ages and Hf isotope compositions of the Mayuan migmatite complex, NW Fujian Province, Southeast China: constraints on the timing and nature of a regional tectonothermal event associated with the Caledonian orogeny. Lithos 119, 163–180.
Liu, Y., Hu, Z., Zong, K., Gao, C., Gao, S., Xu, J., Chen, H., 2010b. Reappraisement and refinement of zircon U-Pb isotope and trace element analyses by LA-ICP-MS. Chinese Science Bulletin 55, 1535–1546.
Ludwig, K.R., 2003. User's manual for Isoplot 3.00: a geochronological toolkit for Microsoft Excel. Berkeley Geochronology Centre Special Publication, p. 74.
McLelland, J.M., Daly, J.S., Chiarenzelli, J., 1993. Sm-Nd and U-Pb isotopic evidence of juvenile crust in the Adirondack lowlands and implications for the evolution of the Adirondack Mts. The Journal of Geology 101, 97–105.
McLennan, S., Bock, B., Compston, W., Hemming, S., McDaniel, D., 2001. Detrital zircon geochronology of Taconian and Acadian foreland sedimentary rocks in New England. Journal of Sedimentary Research 71, 305–317.
Miller, M.M., Saleeby, J.B., 1995. U-Pb geochronology of detrital zircon from Upper Jurassic synorogenic turbidites, Galice Formation, and related rocks, western Klamath Mountains: correlation and Klamath Mountains provenance. Journal of Geophysical Research: Solid Earth (1978–2012) 100, 18045–18058.
Pang, X., Chen, C.-M., Wu, M.-S., He, M., Wu, X.-j., 2006. The Pearl River deep-water fan systems and significant geological events (in Chinese with English abstract). Advances in Earth Science 21, 793–799.
Rainbird, R.H., McNicoll, V., Theriault, R., Heaman, L., Abbott, J., Long, D., Thorkelson, D., 1997. Pan-continental river system draining Grenville Orogen recorded by U-Pb and Sm-Nd geochronology of Neoproterozoic quartzarenites and mudrocks, northwestern Canada. The Journal of Geology 105, 1–17.
Richardson, N.J., Densmore, A.L., Seward, D., Wipf, M., Li, Y., 2011. Did incision of the Three Gorges begin in the Eocene? Reply, Geology 39 (9), e245-e245.
Rino, S., Kon, Y., Sato, W., Maruyama, S., Santosh, M., Zhao, D., 2008. The Grenvillian and Pan-African orogens: world's largest orogenies through geologic time, and their implications on the origin of superplume. Gondwana Research 14, 51–72.
Robinson, R.A.J., Brezina, C.A., Parrish, R.R., Horstwood, M.S.A., Nay Win, O., Bird, M.I., Myint, T., Walters, A.S., Oliver, G.J.H., Khin, Z., 2014. Large rivers and orogens: the evolution of the Yarlung Tsangpo–Irrawaddy system and the eastern Himalayan syntaxis. Gondwana Research 26, 112–121.
Scherer, E., Münker, C., Mezger, K., 2001. Calibration of the lutetium-hafnium clock. Science 293, 683–687.
Seno, T., Stein, S., Gripp, A.E., 1993. A model for the motion of the Philippine Sea Plate consistent with NUVEL-1 and geological data. Journal of Geophysical Research, Solid Earth 98, 17941–17948.
Shao, L., Pang, X., Chen, C.M., Shi, H.S., Li, Q.Y., Qiao, P.J., 2007. Terminal Oligocene sedimentary environments and abrupt provenance change event in the northern South China Sea (in Chinese with English abstract). Geology in China 34, 1022–1031.
Shu, L., 2006. Predevonian tectonic evolution of south China: from Cathaysian Block to Caledonian period folded orogenic belt. Geological Journal of China Universities 12, 418–431.
Sláma, J., Košler, J., Condon, D.J., Crowley, J.L., Gerdes, A., Hanchar, J.M., Horstwood, M.S.A., Morris, G.A., Nasdala, L., Norberg, N., Schaltegger, U., Schoene, B., Tubrett, M.N., Whitehouse, M.J., 2008. Plešovice zircon—a new natural reference material for U-Pb and Hf isotopic microanalysis. Chemical Geology 249, 1–35.
Suppe, J., 1984. Kinematics of arc-continent collision, flipping of subduction, and back-arc spreading near Taiwan. Memoir of the Geological Society of China 6, 21–33.
Tan, L.P., Youh, C.C., 1978. Characteristics and paleogeographic environment of the metamorphosed high-purity sandstone deposits in Taiwan. Proceedings of the Geological Society of China 21, 92–100.
Tapponnier, P., Zhiqin, X., Roger, F., Meyer, B., Arnaud, N., Wittlinger, G., Jingsui, Y., 2001. Oblique stepwise rise and growth of the Tibet Plateau. Science 294, 1671–1677.
Taylor, B., Hayes, D.E., 1980. The tectonic evolution of the South China Basin. The tectonic and geologic evolution of Southeast Asian seas and islands. pp. 89–104.
Teng, L.S., Wang, Y., Tang, C.H., Huang, C.Y., Huang, T.C., Yu, M.S., Ke, A., 1991. Tectonic aspects of the Paleogene depositional basin of northern Taiwan. Proceedings of the Geological Society of China 34, 313–336.
Wan, Y., Liu, D., Xu, M., Zhuang, J., Song, B., Shi, Y., Du, L., 2007. SHRIMP U-Pb zircon geochronology and geochemistry of metavolcanic and metasedimentary rocks in Northwestern Fujian, Cathaysia block, China: tectonic implications and the need to redefine lithostratigraphic units. Gondwana Research 12, 166–183.
Wang, P., 1998. Deformation of Asia and global cooling: searching links between climate and tectonic (in Chinese with English abstract). Quaternary Science 3, 213–221.
Wang, P., 2004. Cenozoic deformation and the history of sea–land interactions in Asia. Geophysical Monograph Series 1–22.
Wang, Q., Wyman, D.A., Li, Z.-X., Bao, Z.W., Zhao, Z.-H., Wang, Y.-X., Jian, P., Yang, Y.-H., Chen, L.-L., 2010. Petrology, geochronology and geochemistry of ca.780 Ma A-type granites in South China: petrogenesis and implications for crustal growth during the breakup of the supercontinent Rodinia. Precambrian Research 178, 185–208.
Wang, E., Kirby, E., Furlong, K.P., van Soest, M., Xu, G., Shi, X., Kamp, P.J.J., Hodges, K.V., 2012. Two-phase growth of high topography in eastern Tibet during the Cenozoic. Nature Geoscience 5, 640–645.
Wong, J., Sun, M., Xing, G., Li, X.-h., Zhao, G., Wong, K., Wu, F., 2011. Zircon U-Pb and Hf isotopic study of Mesozoic felsic rocks from eastern Zhejiang, South China: geochemical contrast between the Yangtze and Cathaysia blocks. Gondwana Research 19, 244–259.
Woodhead, J., Hergt, J., Shelley, M., Eggins, S., Kemp, R., 2004. Zircon Hf-isotope analysis with an excimer laser, depth profiling, ablation of complex geometries, and concomitant age estimation. Chemical Geology 209, 121–135.
Xu, Y.H., Chen, J., 2010. Uranium-lead dating of detrital zircons from the Minjiang and Jiulong Estuaries in the western coast of the Taiwan Strait: implication for its provenance (in Chinese with English abstract). Acta Oceanologica Sinica 32, 110–117.
Xu, X., O'Reilly, S.Y., Griffin, W.L., Wang, X., Pearson, N.J., He, Z., 2007. The crust of Cathaysia: age, assembly and reworking of two terranes. Precambrian Research 158, 51–78.
Yan, Y., Andy, C., Xia, B., Lin, G., Stephanie, B., Hu, X., 2009a. A fission-track and (U–Th)/He thermochronometric study of the northern margin of the South China Sea: an example of a complex passive margin. Tectonophysics 474 (3-4), 584–594.
Yan, Y., Hu, X., Lin, G., Xia, B., Li, X., Patel, R.C., 2009b. Denudation history of South China block and sediment supply to northern margin of the South China Sea. Journal of Earth Science 20, 57–65.
Yan, Y., Carter, A., Palk, C., Brichau, S., Hu, X., 2011. Understanding sedimentation in the Song Hong–Yinggehai Basin, South China Sea. Geochemistry, Geophysics, Geosystems 12 (6), Q06014. http://dx.doi.org/10.1029/2011GC003533.

Yan, Y., Carter, A., Huang, C.Y., Chan, L.S., Hu, X.Q., Lan, Q., 2012. Constraints on Cenozoic regional drainage evolution of SW China from the provenance of the Jianchuan Basin. Geochemistry, Geophysics, Geosystems 13, Q03001. http://dx.doi.org/10.1029/2011GC003803.
Yang, S., Youn, J.S., 2007. Geochemical compositions and provenance discrimination of the central south Yellow Sea sediments. Marine Geology 243, 229–241.
Yang, T.F., Lee, T., Chen, C.-H., Cheng, S.-N., Knittel, U., Punongbayan, R.S., Rasdas, A.R., 1996. A double island arc between Taiwan and Luzon: consequence of ridge subduction. Tectonophysics 258, 85–101.
Yao, B.C., Zeng, W.J., Chen, Y.Z., Zhang, X.L., Hayes, D.E., Diebold, J., Bubl, P., Spangler, S., 1994. The crustal structure in the eastern part of the northern margin of the South China Sea (in Chinese with English abstract). Acta Geophysica Sinica 37 (1), 27–35.
Yokoyama, K., Tsutsumi, Y., Lee, C.S., Shen, J.S., Lan, C.Y., Zhao, L., 2007. Provenance study of tertiary sandstones from the Western foothills and Hsuehshan Range, Taiwan. Bulletin of the National Museum of Nature and Science Series C 33, 7–26.
Yu, J.H., Wang, L., O'Reilly, S.Y., Griffin, W.L., Zhang, M., Li, C., Shu, L., 2009. A Paleoproterozoic orogeny recorded in a long-lived cratonic remnant (Wuyishan terrane), eastern Cathaysia Block, China. Precambrian Research 174, 347–363.
Yu, J.H., O'Reilly, S.Y., Zhou, M.-F., Griffin, W.L., Wang, L., 2012. U-Pb geochronology and Hf–Nd isotopic geochemistry of the Badu Complex, Southeastern China: implications for the Precambrian crustal evolution and paleogeography of the Cathaysia Block. Precambrian Research 222–223, 424–449.
Yuan, H., Gao, S., Dai, M., Zong, C., Gunther, D., Fontaine, G., Liu, X., Diwu, C., 2008. Simultaneous determinations of U-Pb age, Hf isotopes and trace element compositions of zircon by excimer laser-ablation quadrupole and multiple-collector ICP-MS. Chemical Geology 247, 100–118.
Zhang, X.H., 2008. Tectonic Geology in China Seas. Ocean Press, Beijing.
Zhang, J.Y., Yin, A., Liu, W.C., Wu, F.Y., Lin, D., Grove, M., 2012. Coupled U-Pb dating and Hf isotopic analysis of detrital zircon of modern river sand from the Yalu River (Yarlung Tsangpo) drainage system in southern Tibet: constraints on the transport processes and evolution of Himalayan rivers. Geological Society of America Bulletin 124, 1449–1473.
Zheng, H., Clift, P.D., Wang, P., Tada, R., Jia, J., He, M., Jourdan, F., 2013. Pre-Miocene birth of the Yangtze River. Proceedings of the National Academy of Sciences of the United States of America 110, 7556–7561.
Zhong, D., Ding, L., 1996. Rising process of the Qinghai-Xizang (Tibet) Plateau and its mechanism. Science in China (Series D) 39, 369–379.
Zhou, X.M., Li, W.X., 2000. Origin of Late Mesozoic igneous rocks in Southeastern China: implications for lithosphere subduction and underplating of mafic magmas. Tectonophysics 326, 269–287.
Zhou, D., Ru, K., Chen, H.Z., 1995. Kinematics of Cenozoic extension on the South China Sea continental margin and its implications for the tectonic evolution of the region. Tectonophysics 251, 161–177.
Zhou, X.M., Sun, T., Shen, W.Z., Shu, L.S., Niu, Y.L., 2006. Petrogenesis of Mesozoic granitoids and volcanic rocks in South China: a response to tectonic evolution. Episodes 29, 26–33.